Check for updates

CJC Chinese Journal of Chemistry 中国化学 · An International Journal

For submission: https://mc.manuscriptcentral.com/cjoc
For published articles: https://onlinelibrary.wiley.com/journal/16147065

Concise Report

Cite this paper: *Chin. J. Chem.* **2021**, *39*, 1303—1309. **DOI: 10.1002/cjoc.202000725**

A Mitochondria-Specific Orange/Near-Infrared-Emissive Fluorescent Probe for Dual-Imaging of Viscosity and H_2O_2 in Inflammation and Tumor Models

Li Fan,*[a] Qi Zan,[a] Xiaodong Wang,[a] Shuohang Wang,[b] Yuewei Zhang,*[b] Wenjuan Dong,[a] Shaomin Shuang,[a] and Chuan Dong*[a]

[a] *Institute of Environmental Science, College of Chemistry and Chemical Engineering, Shanxi University, Taiyuan, Shanxi 030006, China*
[b] *School of Chemistry and Pharmaceutical Engineering, Jilin Institute of Chemical Technology, Jilin, , Jilin 132022, China*

Keywords

Viscosity | H_2O_2 | Mitochondria-specific | Fluorescent probes | Fluorescence spectroscopy

Main observation and conclusion

Elucidating the intrinsic relationship between viscosity/H_2O_2 and mitochondria-associated diseases remains a great challenge owing to the lack of research on multiple diseases models, such as inflammation and malignant tumor models. In this work, we have developed a mitochondria-specific orange/near-infrared-emissive fluorescent probe **TTPB**, for dual-imaging of viscosity and H_2O_2 levels in two different channels. The probe exhibited a remarkable response to viscosity with NIR emission round 666 nm, and was highly sensitive to H_2O_2 in orange channel with emission peak at 586 nm. Moreover, **TTPB** has good mitochondria-specific ability and permits individual detecting of viscosity in NIR channels and H_2O_2 levels in orange channel in living cells. More notably, **TTPB** was successfully applied to simultaneously image the viscosity and H_2O_2 levels in inflammation and cancer models.

Comprehensive Graphic Content

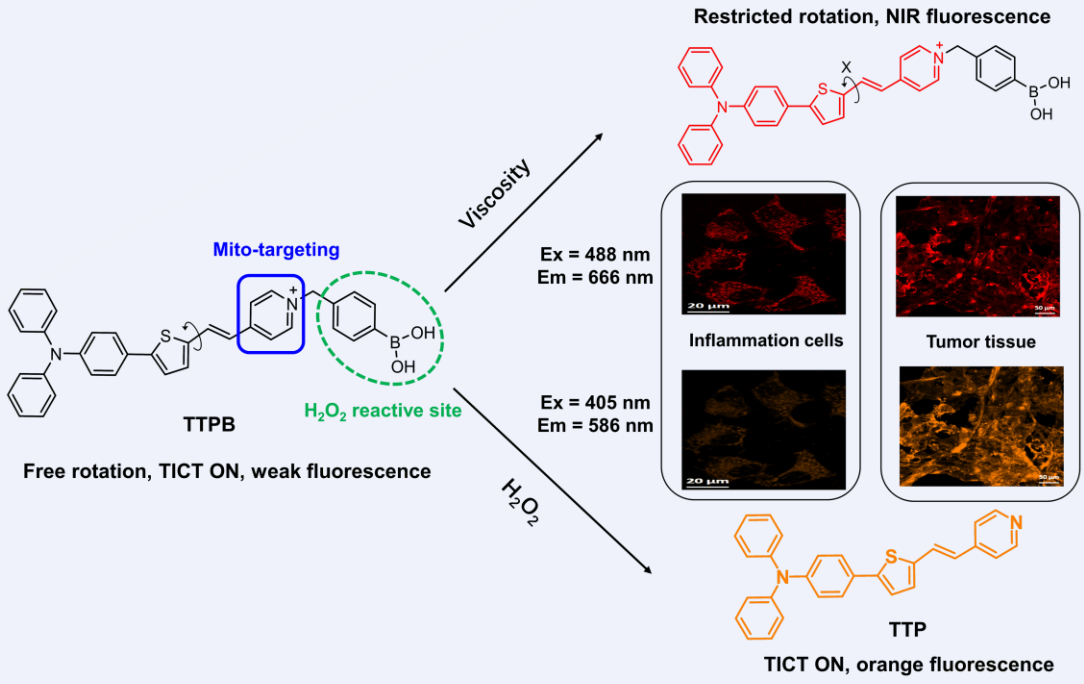

*E-mail: fanli128@sxu.edu.cn; zhangyueweichem@163.com; dc@sxu.edu.cn

View HTML Article | Supporting Information

© 2021 SIOC, CAS, Shanghai, & WILEY-VCH GmbH

Background and Originality Content

Cellular viscosity, as an essential micro-environmental parameter, plays a critical role in many diffusion-mediated biological processes, such as signal transport, electron transport and so on.[1] Mitochondria, serving as the cellular power workshop, are closely linked to cellular viability and physiological activity.[2] Abnormal viscosity changes can cause mutations in mitochondrial network organization, and subsequently affect metabolite diffusion, which have been found to associate with inflammation, diabetes, neurodegenerative disease and even cancer.[3]

As a prominent member of reactive oxygen species (ROS), hydrogen peroxide (H_2O_2) is mainly propagated within mitochondria, and plays regulatory roles in cell growth, immune response, host defense as well as signaling pathways.[4-5] However, the aberrant production or accumulation of H_2O_2 within mitochondria can induce mitochondrial swelling, fracture and fine structure mutation, thereby leading to mitochondria malfunction and some diseases, including cancer, inflammatory, obesity as well as neurodegenerative diseases.[6-8] To better understand the internal relationship between the levels of mitochondrial viscosity/H_2O_2 and mitochondria-associated diseases, it is urgently need to exploit a simple but reliable and precise strategy for dual-detection of mitochondrial viscosity and H_2O_2 changes *in vivo*.

Fluorescent probes in combination with fluorescence imaging technology have become the powerful tools for detecting biomolecules and biological parameters in live samples, because of their simple operation, high sensitivity, excellent spatiotemporal resolution and non-disruptive nature. So far, a lot of outstanding fluorescent probes for single-imaging mitochondrial viscosity or H_2O_2 have been reported,[9-29] yet they could not simultaneously detect the two markers. Compared with the combination of several fluorescent probes in one system, a single probe with dual-sensing ability can avoid the spectral cross-talk, different localizations and metabolism of these probes.[30] In 2017, Lin's group designed a single fluorescent probe (Mito-VH) based on styrylpyridine fluorophore, for dual-detection of viscosity and H_2O_2 in mitochondria with different imaging channels in living cells for the first time.[20] However, this probe possessed a short emission wavelength and small Stokes shifts, which might suffer from excessive autofluorescence in living systems and shallow penetration depth. Subsequently, Huang *et al*. synthesized a two-photo fluorescent probe (Mito-LX) with a dual-response towards changes in the viscosity within near-infrared (NIR) emission and H_2O_2 in visible channel in mitochondria, and extended the application into Parkinson's disease models.[28] Very recently, Liu and coworkers reported a single NIR fluorescent probe with a large Stokes shift for simultaneous imaging of mitochondrial viscosity and H_2O_2 in Alzheimer's disease models.[31] To the best of our knowledge, only these three dual-imaging fluorescent probes have been developed for monitoring both mitochondrial viscosity and H_2O_2, and the limited diseases models prevent us from delving into the intrinsic relationship between viscosity/H_2O_2 and mitochondria-associated diseases due to the lack of suitable fluorescent probes and research on multiple diseases models, such as inflammation and malignant tumor models.

In this contribution, we designed a single orange/near-infrared-emissive fluorescent probe (**TTPB**, Scheme 1) for dual-imaging of viscosity and H_2O_2 within mitochondria. **TTPB** is comprised by a pyridinium cation (electron acceptor moiety, A), a phenylboronic acid unit, an ethylene (π-bridge), a thiophene fragment (π-bridge and electron donor group, D), and a triphenylamine segment (D), indicating a typical D-π-A molecular configuration, therefore leading to NIR fluorescence emission. The pyridinium cation was well-known as a mitochondrial-specific motif owing to the electrostatic interaction with the negative membranes potential in mitochondria. The phenylboronic acid was chosen as the H_2O_2 reactive unit in dual-sensing H_2O_2/viscosity for the first time, while the reported single probes employed phenylborate ester as H_2O_2-sensitive group.[20,28,31] Meanwhile, the triphenylamine combined with thiophene acted as the viscosity-sensitive unit due to the more rotations than that in the reported single probes for dual-sensing H_2O_2/viscosity,[20,28,31] which was predicted to display a high sensitive response to viscosity. The detailed synthetic route for probing **TTPB** and **TTP** was shown in Scheme 2, and the structures were fully characterized by ^{1}H NMR, ^{13}C NMR and HR-MS in the Supporting Information. As expected, in a non-viscous or low-viscous environment, the molecule (**TTPB**) is in a twisted intramolecular charge transfer (TICT) state due to the free rotations, resulting in the non-radiative decay of the excited state and the non/weak fluorescence emission. However, as the high-viscosity solvent presents, the rotations are restricted and the TICT state is inhibited, leading to efficient conjugation of the molecule and further the enhancement of near-infrared (NIR) fluorescence emission. On the other hand, after the addition of H_2O_2, the arylboronic acid in **TTPB** is deprotected to phenol, followed by an elimination reaction to give **TTP**, which exhibits a remarked orange fluorescent emission due to the inhibition of the TICT process. We then demonstrated in detail the ability of **TTPB** for imaging mitochondrial viscosity and H_2O_2 changes individually in living cells. Besides, **TTPB** was successfully applied to simultaneously monitor the variation of mitochondrial viscosity and H_2O_2 in inflammation or malignant tumor models.

Scheme 1 The structure and mechanism of **TTPB** for dual-responding to mitochondrial viscosity and H_2O_2

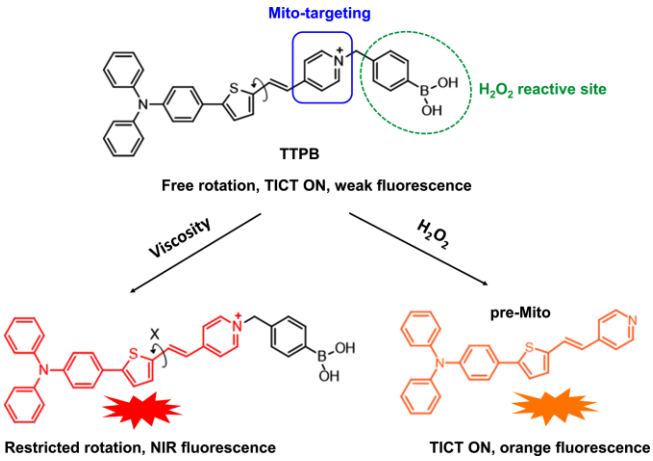

Scheme 2 The synthetic route of **TTPB** and **TTP**

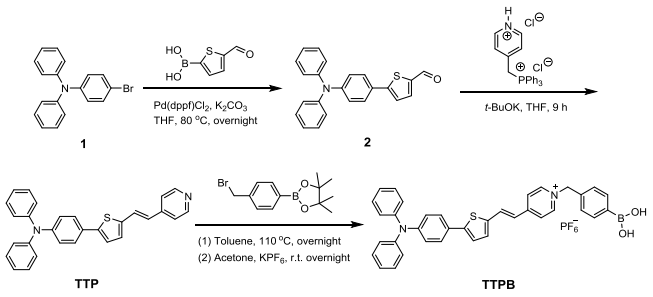

Results and Discussion

Spectroscopic response of TTPB to viscosity

The optical response of **TTPB** to viscosity was performed by measuring their absorbance and emission spectra in methanol

 © 2021 SIOC, CAS, Shanghai, & WILEY-VCH GmbH

and glycerol, respectively. As shown in Figure S1 and Table S1, **TTPB** exhibited a maximum absorption at 488 nm (ε_{488} = 3.472 × 10^4 L·mol^{-1}·cm^{-1}) in pure methanol, while red-shifted to 502 nm (ε_{502} = 2.910 × 10^4 L·mol^{-1}·cm^{-1}) in 99% glycerol. To precisely identify the viscosity-sensitive behavior of **TTPB**, the fluorescence spectra of **TTPB** in methanol/glycerol mixtures were recorded (Figure 1a), where the viscosity levels (cP) were tuned by adjusting the glycerol fraction (f_G). Upon increasing the viscosity from 0.59 cP (0% glycerol) to 950 cP (99% glycerol), a significant emission enhancement was observed at 666 nm, suggesting **TTPB** could be potentially used as a NIR-emissive viscosimeter for bioimaging with minimum autofluorescence and photo damage. Meanwhile, the fluorescent color changed from light-pink to red (Inset of Figure 1a). The viscosity-dependent property of **TTPB** might be attributed to the fact that the rotations of the molecule were restricted and the TICT state was inhibited in high viscous environment (Scheme 1). Interestingly, according to the Förster-Hoffmann equation, a plot of log I_{666} vs log η was linear over the viscosity range from 0.59 to 950 cP (R^2 = 0.9909, slope = 0.3725) (Figure 1b), indicating the high sensitivity of **TTPB** to micro-viscosity changes. Meanwhile, **TTPB** had a remarkably large Stokes shift of 178 nm that could effectively reduce the excitation interference. Subsequently, the fluorescence quantum yield (QY) of **TTPB** in different methanol/glycerol mixtures (glycerol from 0% to 99%) was investigated. As shown in Table S1, the QY value of **TTPB** was only 0.55% in pure methanol (0.59 cP), whereas it reached up to 8.06% in 99% glycerol (950 cP) solution. Additionally, the fluorescence lifetimes of **TTPB** in different methanol/glycerol mixtures also exhibited a similar variation tendency toward viscosity (Figure S2), further comfirming the viscosity-sensitive feature of **TTPB.**

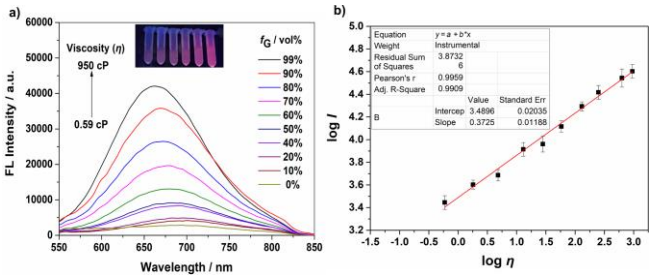

Figure 1 (a) Fluorescence spectral changes of **TTPB** (5 μmol/L) in different methanol/glycerol mixtures (glycerol from 0% to 99%), excited at 488 nm. Inset: the fluorescent colour of the solution changed from light-pink to red. (b) The linear relationship between log *I* and log *η* in the range of *η* = 0.59 cP to *η* = 950 cP.

Furthermore, we confirmed that **TTPB** was highly selective toward viscosity change in the presence of various polarities solvents, including glycerol, ethanol, water, methanol, DMSO and acetonitrile (Figure S3), and was insensitive to changes in pH ranging from 3.0—10.0, in methanol/glycerol with glycerol 0% or 90% (Figure S4), indicating the high selectivity of **TTPB** toward viscosity changes.

Spectroscopic response of TTPB to H_2O_2

To verify whether **TTPB** was responsive to H_2O_2 as designed, the optical properties of probe **TTPB** and **TTP** were measured in the absence and presence of H_2O_2. **TTPB** itself displayed a maximum absorption around 485 nm (ε_{485} = 2.845 × 10^4 L·mol^{-1}·cm^{-1}), while reacting with H_2O_2, the maximum absorption blue-shifted to 408 nm (ε_{408} = 2.434 × 10^4 L·mol^{-1}·cm^{-1}), which was similar to that of **TTP** (ε_{408} = 2.549 × 10^4 L·mol^{-1}·cm^{-1}) (Figure S5). Figure 2 depicted the fluorescence emission spectra of **TTPB** to various H_2O_2 levels. When adding the concentrations of H_2O_2 from 0 to 100 μmol/L, the fluorescence emission at 586 nm exhibited a dramatic increase and the fluorescent color of the solutions turned to bright orange. Notably, there was about 80 nm emission shift between the emission peak of the response to viscosity and that response to H_2O_2, which was beneficial for **TTPB** to fluorescence image the viscosity and H_2O_2 in different channels. Additionally, an excellent linear relationship between the fluorescence intensity (I_{586}) and the H_2O_2 concentrations was established over the range of 0—30 μmol/L (R^2 = 0.9891, Figure 2b), and the detection limit was calculated as 0.141 μmol/L (3σ/slope method), which is much lower than physiological H_2O_2 level of the organization in inflammation state (10—100 μmol/L).[32]

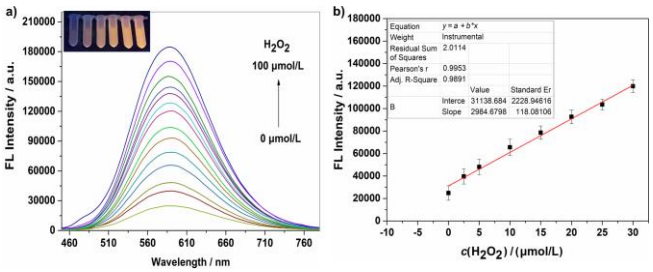

Figure 2 (a) Fluorescence response of **TTPB** (5 μmol/L) to various concentrations of H_2O_2 (0-100 μmol/L) in DMSO/PBS (1/1, *V*/*V*, pH 8.4), excited at 405 nm. (b) The linear relationship between the fluorescence intensity at 588 nm and H_2O_2 concentration in the range of 0—30 μmol/L.

We then demonstrated that **TTPB** was highly selective for H_2O_2 change in complex biological matrixes (Figure S6), and exhibited significant fluorescence enhancement around pH 8.4 within the alkaline mitochondrial matrix environment (pH ~8.0) (Figure S7). We further confirmed the response mechanism of **TTPB** to H_2O_2 (proposed in Scheme 1), on the base of high resolution mass spectrometry (HR-MS) analysis (Figure S8). After reaction of **TTPB** with H_2O_2, the mass peak at *m*/*z* = 565.2110 ([**TTPB**]$^+$, calcd: 565.2116) for free **TTPB** disappeared, while a new peak at *m*/*z* = 431.1587 corresponding to the formation of adduct ([**TTPB**-H_2O_2]$^+$) was observed, which was very similar to **TTP** ([**TTP**]$^+$, calcd: 431.1576).

Mitochondria-specific ability of TTPB

To confirm the mitochondria-specific ability of **TTPB**, a co-localization experiment between **TTPB** and MitoTracker Deep Red (MTDR, a mitochondria-specific dye) was performed. As expected, **TTPB** exhibited clear filament morphologies (Figure 3a) and matched well with MTDR (Figures 3b, 3c), with an average Pearson's co-localization coefficient (PC) as high as 0.94 (Figure 3d). On the contrary, **TTPB** co-stained with LysoBrite NIR (LB-NIR, a commercial lysosome-specific dye) displayed poor co-localization imaging, with a low PC of 0.13 (Figures 3e—3h). These results suggested that **TTPB** predominantly localized in the mitochondria. Moreover, a *CCK-8* assay demonstrated the non-toxicity of **TTPB** to live cells under the imaging conditions (Figure S9), and the IC_{50} value was calculated to be 47.44 μmol/L.

Fluorescence imaging of TTPB to viscosity in live cells

With its highly viscosity-sensitive *in vitro* and excellent mitochondria-specific ability confirmed, **TTPB** was investigated for its viscosity-dependent fluorescence response in live cells. As reported, the ionophores (nystatin and monensin) can cause structural changes and swelling of mitochondria, further leading to mitochondrial malfunction accompanied by mitochondrial viscosity changes.[28] After incubating with **TTPB** for 30 min, HeLa cells were further treated by nystatin or monensin for another 30 min, respectively. As depicted in Figure 4, the cells treated with

 © 2021 SIOC, CAS, Shanghai, & WILEY-VCH GmbH

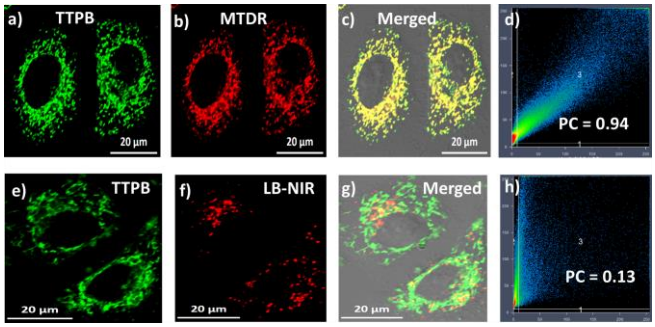

Figure 3 Fluorescence images of HeLa cells co-stained with (a, e) **TTPB** (5 μmol/L, 30 min) and (b) MTDR (0.3 μmol/L, 30 min) or (f) LB-NIR (0.3 μmol/L, 30 min) for 30 min, respectively. (c, g) Merged images. (d) The Pearson's co-localization correlation of **TTPB** with MTDR intensities (PC = 0.94), and (h) the Pearson's co-localization correlation of **TTPB** with LB-NIR intensities (PC = 0.13). **TTPB**: λ_{ex} = 488 nm, λ_{em} = 560—670 nm; MTDR and LB-NIR: λ_{ex} = 633 nm, λ_{em} = 680—770 nm. Scale bar: 20 μm.

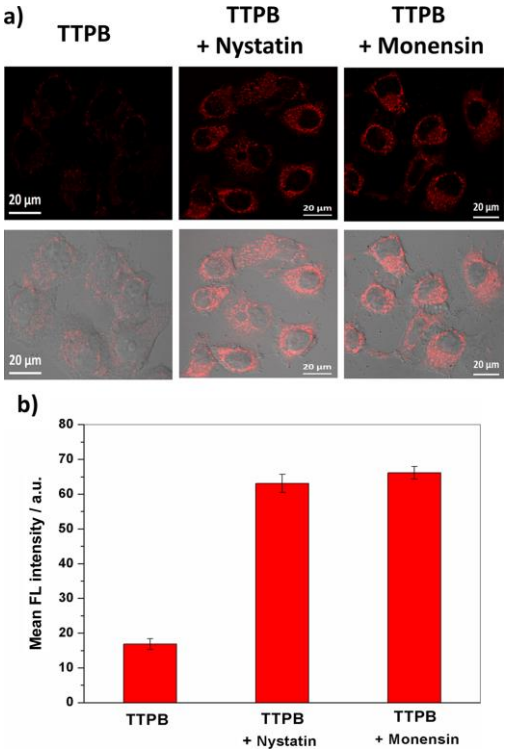

Figure 4 (a) Fluorescence images of HeLa cells incubated with **TTPB** (5 μmol/L, 30 min), and then treated without or with nystatin (10 μmol/L, 30 min) or monensin (10 μmol/L, 30 min). (b) The mean fluorescence intensities of images shown in (a). Error bars represent mean deviation (± S.D.), n = 3. NIR channel for **TTPB**: λ_{ex} = 488 nm, λ_{em} = 650—740 nm. Scale bar: 20 μm.

TTPB only displayed dim fluorescence in the NIR channel (650-740 nm), while the fluorescence intensity in nystatin or monensin treated cells obviously enhanced, indicating a viscosity rise in mitochondria, and the ability of **TTPB** for monitor mitochondrial viscosity fluctuations.

Fluorescence imaging of TTPB to H_2O_2 in living cells

The potential ability of **TTPB** to visualize H_2O_2 in live cells was further investigated upon varying stimulation. As illustrated in Figure 5, compared with only **TTPB**-stained cells, the fluorescence emission within H_2O_2-treated cells showed a remarkable fluorescence enhancement in the orange channel (540—640 nm), indicating the ability of **TTPB** for imaging exogenous H_2O_2 in live cells. We then examine whether **TTPB** could visualize endogenous H_2O_2, by adding phorbol myristate acetate (PMA) or rotenone (ROT), which can promote cellular ROS levels.[28,31] As predicted, a dramatic fluorescence enhancement was observed upon PMA or ROT induction. Remarkably, the following addition of N-acetyl-*L*-cysteine (NAC, an efficient ROS scavenger), almost quenched the fluorescence signals in the orange channel. Thus, the results suggested that **TTPB** could detect both exogenous and endogenous H_2O_2 in live cells.

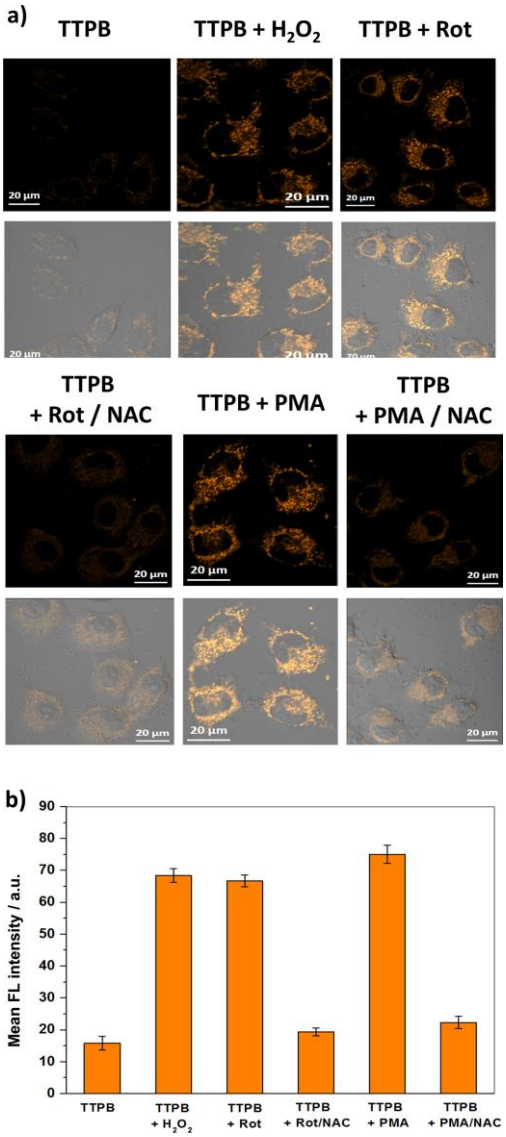

Figure 5 (a) Fluorescence images of HeLa cells incubated with **TTPB** (5 μmol/L, 30 min), and then treated without and with H_2O_2 (100 μmol/L, 40 min), rot (5 μmol/L, 40 min), rot (5 μmol/L, 40 min) with NAC (50 μmol/L, 40 min), PMA (5 μg/mL, 40 min) or PMA (5 μg/mL, 40 min) with NAC (50 μmol/L, 40 min). The mean fluorescence intensities of images shown in (a). Error bars represent mean deviation (± S.D.), n = 3. Orange channel for **TTPB**: λ_{ex} = 405 nm, λ_{em} = 540—640 nm. Scale bar: 20 μm.

Dual-imaging of viscosity and H_2O_2 in inflammation model

Having verified the ability of **TTPB** to separately image mitochondrial viscosity and H_2O_2 in two different channels, we then evaluate its capability of simultaneously tracking mitochondrial viscosity and H_2O_2 in an inflammation model induced by lipopolysaccharide (LPS), which has been verified to trigger cells to pro-

 © 2021 SIOC, CAS, Shanghai, & WILEY-VCH GmbH

duce inflammation.[33-34]

As illustrated in Figure 6, the **TTPB**-stained cells showed faint fluorescence in both orange channel (for H_2O_2) and NIR channel (for viscosity), while obvious enhanced fluorescence were observed in both of the two channels, implying the increase in pH viscosity and H_2O_2 in the LPS-mediated inflammatory cells. The results suggested that **TTPB** holds great potential for dual-imaging viscosity and H_2O_2 levels in pathogenic cells.

Dual-imaging of viscosity and H_2O_2 in malignant tumor model

Building on the prominent results from live cells imaging, **TTPB** was finally applied to simultaneously monitor H_2O_2 level and viscosity in live tissues slices. Specifically, the normal tissues (including heart, liver, spleen, lung, kidney and thymus) and tumor tissue were treated with **TTPB** for 30 min, respectively. Obviously, in comparison with the very dim fluorescence signals from normal tissues (Figure 7 and Figure S10), the tumor tissue exhibited

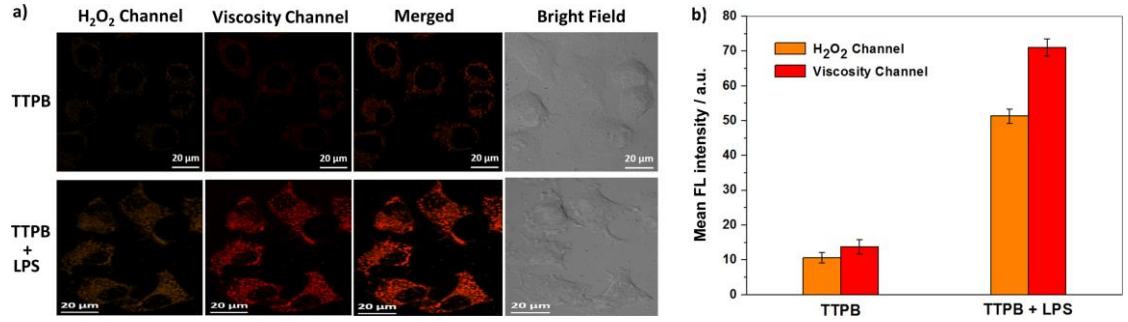

Figure 6 (a) Fluorescence dual-images of HeLa cells incubated with **TTPB** (5 μmol/L, 30 min), and then treated without or with LPS (100 μg/mL, 2h). (b) The mean fluorescence intensities of images shown in (a). Error bars represent mean deviation (± S.D.), n = 3. Orange channel (H_2O_2 channel): λ_{ex} = 405 nm, λ_{em} = 540—640 nm. NIR channel (viscosity channel): λ_{ex} = 488 nm, λ_{em} = 650—740 nm. Scale bar: 20 μm.

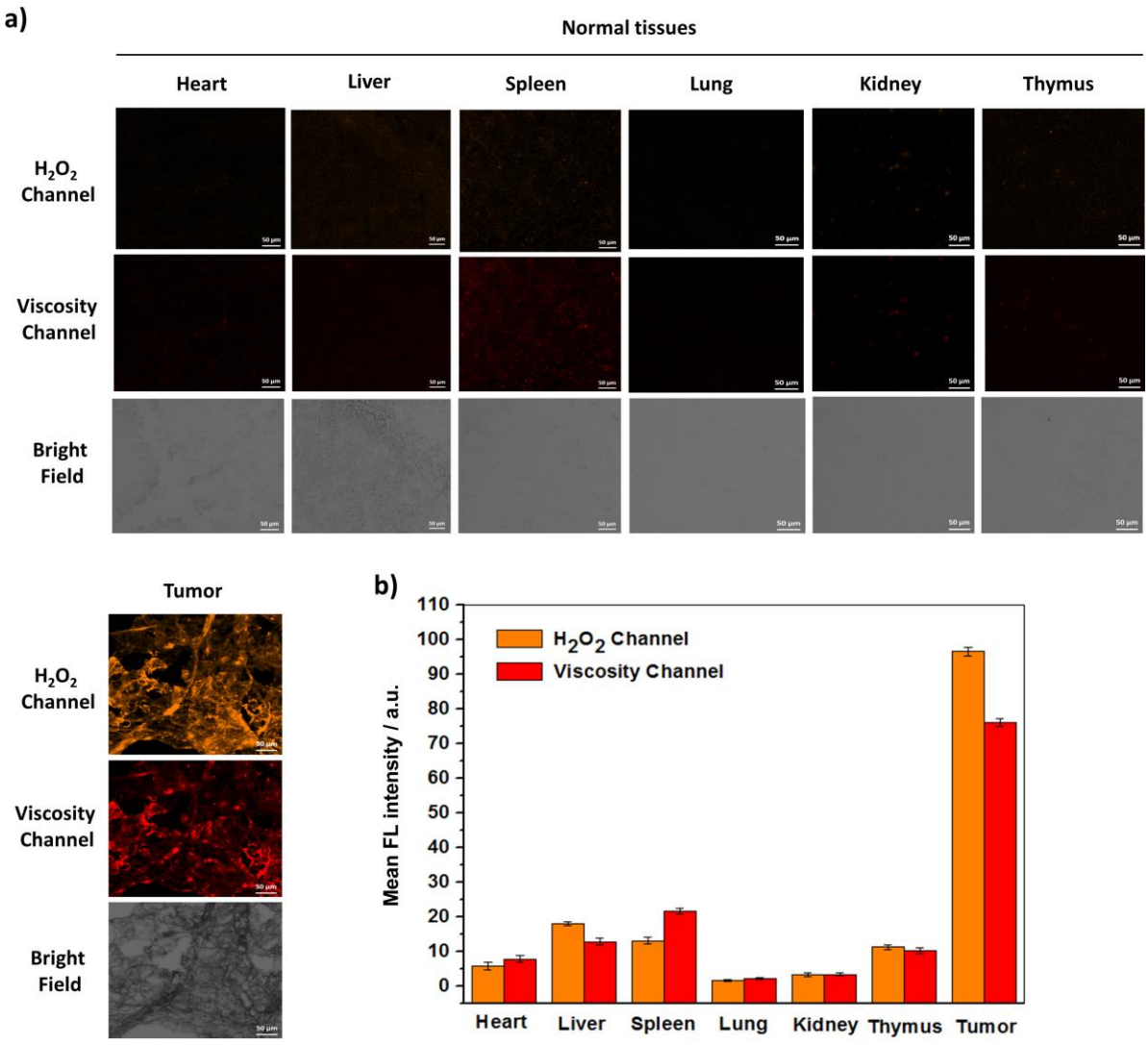

Figure 7 (a) Fluorescence dual-images of **TTPB** (10 μmol/L, 30 min) in living normal tissues and tumor. (b) The mean fluorescence intensities of images shown in (a). Error bars represent mean deviation (± S.D.), n = 3. Orange channel (H_2O_2 channel): λ_{ex} = 405 nm, λ_{em} = 540—640 nm. NIR channel (viscosity channel): λ_{ex} = 488 nm, λ_{em} = 650—740 nm. Scale bar: 50 μm.

 © 2021 SIOC, CAS, Shanghai, & WILEY-VCH GmbH

significantly enhanced fluorescence in both orange channel (for H_2O_2) and NIR channel (for viscosity), implying the elevated H_2O_2 level and increased viscosity of tumor tissue. Taken together, the results vividly illustrated that **TTPB** could penetrate into the tissues, and dual-image the contents of viscosity and H_2O_2 in malignant tumor models.

Conclusions

In summary, a mitochondria-specific orange/near-infrared-emissive fluorescent probe **TTPB** was developed for simultaneously imaging the viscosity and H_2O_2 levels in inflammation and cancer models. The probe emitted NIR emission at about 666 nm, and exhibited a good linear relationship over the viscosity range from 0.59 to 950 cP. Meanwhile, **TTPB** displayed high selective and sensitive response to H_2O_2 levels with orange emission around 586 nm. Moreover, we revealed that **TTPB** has satisfactory mitochondria-specific ability and permits the visual monitoring of viscosity and H_2O_2 changes in different channels in live cells. Most importantly, using the single probe **TTPB**, we demonstrated the simultaneous rise of viscosity and H_2O_2 levels in inflammation and tumors models for the first time. Therefore, we believe that the fluorescence probe will be a potential imaging tool for investigating mitochondria-associated diseases.

Experimental

Materials and apparatus

The reagents, apparatus and methods in the work were listed in Supporting Information. The synthetic route of **TTPB** and **TTP** was illustrated in Scheme 2, and the detailed synthesis process and characterizations were shown in the Supporting Information.

Spectroscopic response of TTPB to viscosity

TTPB (1.0 mmol/L) was prepared in DMSO to obtain the stock solution. The solvents were obtained by mixing a methanol/glycerol system in different proportions. The solutions of **TTPB** of different viscosity were prepared by adding the stock solution (1.0 mmol/L) 10 μL to 2 mL of methanol/glycerol system to obtain the final concentration of Mito-TPB (5.0 μmol/L). These solutions were sonicated for 10 min to eliminate air bubbles. Excitation and emission bandwidths were both set at 2.0 nm, and the excitation wavelength was fixed at 405 nm.

Spectroscopic response of TTPB to H_2O_2

5 μmol/L **TTPB** was used in spectroscopic determination by addition of 10 μL stock solution (1.0 mmol/L) to 2.0 mL PBS containing 50% DMSO (pH 8.4). Absorption and emission spectra were recorded after the test solution was incubated at 37 °C for 2 h with H_2O_2. Excitation and emission bandwidths were both set at 2.0 nm, and the excitation wavelength was fixed at 488 nm.

Cell culture and cell cytotoxicity assay

The cell culture and cell cytotoxicity assay conditions were listed in Supporting Information.

Cell imaging experiment

For co-localization experiments. HeLa cells were stained with 5 μmol/L **TTPB** for 30 min at 37 °C, and then co-incubated with 0.3 μmol/L MitoTracker Deep Red or 0.3 μmol/L LysoBrite NIR for further 30 min, respectively. The fluorescence images were carried out on a confocal laser scanning microscope (Zeiss, LSM880) with green channel (λ_{ex} = 488 nm, λ_{em} = 560—670 nm) for **TTPB**, red channel (λ_{ex} = 633 nm, λ_{em} = 680—770 nm) for MitoTracker Deep Red or LysoBrite NIR, respectively.

For imaging of viscosity in live cells. HeLa cells were incubated with **TTPB** (5 μmol/L) for 30 min at 37 °C, and then treated with ionophores (nystatin or monensin) (10 μmol/L) for another 30 min, respectively. The fluorescence images were acquired through a confocal laser scanning microscope (Zeiss, LSM880) with NIR channel (λ_{ex} = 488 nm, λ_{em} = 650—740 nm).

For imaging of H_2O_2 in live cells. HeLa cells were incubated with **TTPB** (5 μmol/L) for 30 min at 37 °C, and then treated with H_2O_2 (100 μmol/L), rot (5 μmol/L), rot (5 μmol/L) + NAC (50 μmol/L), PMA (5 μg/mL), or PMA (5 μg/mL) + NAC (50 μmol/L) for another 40 min, respectively. The fluorescence images were acquired through a confocal laser scanning microscope (Zeiss, LSM880) with orange channel (λ_{ex} = 405nm, λ_{em} = 540—640 nm).

For dual-imaging of H_2O_2 and viscosity in inflammation model. For dual-detection of H_2O_2 and viscosity, the HeLa cells were incubated with **TTPB** (5 μmol/L) for 30 min, and then treated with LPS (100 μg/mL) for 2 h. The fluorescence images were acquired through a confocal laser scanning microscope (Zeiss, LSM880) with orange channel (λ_{ex} = 405 nm, λ_{em} = 540—640 nm) and NIR channel (λ_{ex} = 488 nm, λ_{em} = 650—740 nm).

Tissue slices imaging experiment

KM mice (18—20 g) were purchased from Laboratory Animal Center of Shanxi Cancer Hospital (Taiyuan, China) for in tissue slices experiment. Herein, H22 cells were subcutaneously injected into the right axillae of KM mice, and the tumor was obtained after 12 d. For tissue slices imaging, the normal organs (heart, spleen, liver, lung, kidney and thymus) and tumor were isolated from the mice, then sectioned as 4 μm thicknesses. These slices were incubated with **TTPB** (10 μmol/L) for 30 min, respectively, and finally subjected for fluorescence imaging through a confocal laser scanning microscope (Zeiss, LSM880) with orange channel (λ_{ex} = 405 nm, λ_{em} = 540—640 nm) and NIR channel (λ_{ex} = 488 nm, λ_{em} = 650—740 nm).

Supporting Information

The supporting information for this article is available on the WWW under https://doi.org/10.1002/cjoc.202000725.

Acknowledgement

This work was supported by the National Natural Science Foundation of China (Nos. 81901814 and 21874087) and Natural Science Foundation of Shanxi Province (No. 201801D121040). The animal experiments were approved by the Animal Care and Use Committee of Shanxi University, and performed in compliance with the Animal Management Rules of the Ministry of Health of the People's Republic of China (Document no. 55, 2001).

References

[1] Singer, S. J.; Nicolson, G. L. The fluid mosaic model of the structure of cell membranes. *Science* **1972**, *175*, 720–731.
[2] Ow, Y. L. P.; Green, D. R.; Hao, Z. Y.; Mak, T. W. Cytochrome c: functions beyond respiration. *Nat. Rev. Mol. Cell. Bio.* **2008**, *9*, 532–542.
[3] Stutts, M. J.; Canessa, C. M.; Olsen, J. C. CFTR as a cAMP-dependent regulator of sodium channels. *Science* **1995**, *269*, 847–850.
[4] Kamata, H.; Honda, S.; Maeda, S.; Chang, L.; Hirata, H.; Michael, K. Reactive oxygen species promote TNFα-induced death and sustained JNK activation by Inhibiting MAP kinase phosphatases. *Cell* **2005**, *120*, 649–661.
[5] Jendrach, M.; Mai, S.; Pohl, S. Short- and long-term alterations of mitochondrial morphology, dynamics and mtDNA after transient oxidative stress. *Mitochondrion* **2008**, *8*, 293–304.
[6] Finkel, T.; Serrano, M.; Blasco, M. A. The common biology of cancer and ageing. *Nature* **2007**, *448*, 767–774.

 © 2021 SIOC, CAS, Shanghai, & WILEY-VCH GmbH

[7] Silzer, T. K.; Phillips, N. R. Etiology of type 2 diabetes and Alzheimer's disease: Exploring the mitochondria. *Mitochondrion* **2018**, *43*, 16–24.
[8] Barnham, K. J.; Masters, C. L.; Bush, A. I. Neurodegenerative diseases and oxidative stress. *Nat. Rev. Drug. Discov*. **2004**, *3*, 205–214.
[9] Yang, Z.; He, Y.; Lee, J. H.; Park, N.; Suh, M.; Chae, W. S.; Kim, J. S. A self-calibrating bipartite viscosity sensor for mitochondria. *J. Am. Chem. Soc*. **2013**, *135*, 9181–9185.
[10] Yang, Z. G.; Cao, G. F.; He, Y. X.; Yang, J. H.; Kim, T.; Peng, X. J.; Kim, J. S. Macro-/micro-environment-sensitive chemosensing and biological imaging. *Chem. Soc. Rev*. **2014**, *43*, 4563–4601.
[11] Wen, Y.; Liu, K.; Yang, H.; Liu, Y.; Chen, L.; Liu, Z.; Yi, T. Mitochondria-directed fluorescent probe for the detection of hydrogen peroxide near mitochondrial DNA. *Anal. Chem*. **2015**, *87*, 10579–10584.
[12] Roopa, N.; Kumar, V.; Bhalla, M.; Kumar. Development and sensing applications of fluorescent motifs within the mitochondrial environment. *Chem. Commun*. **2015**, *51*, 15614–15628.
[13] Zhu, H.; Fan, J.; Du, J.; Peng, X. Fluorescent probes for sensing and imaging within specific cellular organelles. *Acc. Chem. Res.* **2016**, *49*, 2115–2126.
[14] Lee, S. C.; Heo, J.; Ryu, J. W.; Lee, C. L.; Kim, S.; Tae, J. S.; Rhee, B. O.; Kim, S. W.; Kwon, O. P. Pyrrolic molecular rotors acting as viscosity sensors with high fluorescence contrast. *Chem. Commun*. **2016**, *52*, 13695–13698.
[15] Baek, Y.; Park, S. J.; Zhou, X.; Kim, G.; Kim, H. M.; Yoon, J. A viscosity sensitive fluorescent dye for real-time monitoring of mitochondria transport in neurons. *Biosens. Bioelectron*. **2016**, *86*, 885–891.
[16] Li, H.; Yao, Q.; Fan, J.; Du, J.; Wang, J.; Peng, X. A two-photon NIR-to-NIR fluorescent probe for imaging hydrogen peroxide in living cells. *Biosens. Bioelectron*. **2017**, *94*, 536–543.
[17] Wen, Y.; Huo, F. J.; Yin, C. X. Organelle targetable fluorescent probes for hydrogen peroxide. *Chin. Chem. Lett*. **2019**, *30*, 1834–1842.
[18] Xu, L. F.; Sun, L. H.; Zeng, F.; Wu, S. Z. Near-infrared fluorescent nanoprobe for detecting hydrogen peroxide in inflammation and ischemic kidney injury. *Chin. J. Chem.* **2020**, *38*, 1304–1310.
[19] Jiang, N.; Fan, J. L.; Zhang, S.; Wu, T.; Wang, J. Y.; Gao, P.; Qu, J.; Zhou, F.; Peng, X. J. Dual mode monitoring probe for mitochondrial viscosity in single cell. *Sens. Actuat. B-Chem.* **2014**, *190*, 685–693.
[20] Ren, M. G.; Deng, B. B.; Zhou, K.; Kong, X. Q.; Wang, J. Y.; Lin, W. Y. Single Fluorescent Probe for Dual-imaging viscosity and H_2O_2 in mitochondria with different fluorescence signals in living cells. *Anal. Chem.* **2017**, *89*, 552–555.
[21] Lee, S. C.; Heo, J.; Woo, H. C.; Lee, J. A.; Seo, Y. H.; Lee, C. L.; Kim, S.; Kwon, O. P. Fluorescent molecular rotors for viscosity sensors. *Chem. Eur. J.* **2018**, *24*, 13706–13718.
[22] Sánchez, A. J.; Lei, E. K.; Kelley, S. O. A multifunctional chemical probe for the measurement of local micropolarity and microviscosity in mitochondria. *Angew. Chem. Int. Ed.* **2018**, *57*, 8891–8895.
[23] Li, S. J.; Li, Y. F.; Liu, H. W.; Zhou, D. Y.; Jiang, W. L.; Yang, J. O.; Li, C. Y. A Dual-response fluorescent probe for the detection of viscosity and H_2S and Its application in studying their cross-talk influence in mitochondria. *Anal. Chem*. **2018**, *90*, 9418–9425.
[24] Zhang, Y. Y.; Li, Z.; Hu, W.; Liu, Z. H. A mitochondrial-targeting near-infrared fluorescent probe for visualizing and monitoring viscosity in live cells and tissues. *Anal. Chem*. **2019**, *91*, 10302–10309.
[25] Sun, C.; Cao, W. F.; Zhang, W.; Zhang, L. L.; Feng, Y.; Fang, M.; Xu, G. Y.; Shao, Z. L.; Yang, X. L.; Meng, X. M. Design of a ratiometric two-photon fluorescent probe for dual-response of mitochondrial SO_2 derivatives and viscosity in cells and in vivo. *Dyes. Pigm.* **2019**, *171*, 107709.
[26] Zou, Z.; Yan, Q.; Ai, S. X.; Qi, P.; Yang, H.; Zhang, Y. F.; Qing, Z. F.; Zhang, L. H.; Feng, F.; Yang, R. H. Real-time visualizing mitophagy-specific viscosity dynamic by mitochondria-anchored molecular rotor. *Anal. Chem*. **2019**, *91*, 8574–8581.
[27] Yang, X. Z.; Xu, B.; Shen, L.; Sun, R.; Xu, Y. J.; Song, Y. L.; Ge, J. F. Series of mitochondria/lysosomes self-targetable near-infrared Hemicyanine Dyes for viscosity detection. *Anal. Chem.* **2020**, *92*, 3517–3521.
[28] Li, S. J.; Wang, P. P.; Feng, W. Q.; Xiang, Y. H.; Dou, K.; Liu, Z. H. Simultaneous imaging of mitochondrial viscosity and hydrogen peroxide in Alzheimer's disease by a single near-infrared fluorescent probe with a large Stokes shift. *Chem. Commun.* **2020**, *56*, 1050–1053.
[29] Ma, C. G.; Sun, W.; Xu, L. M.; Qian, Y.; Dai, J. N.; Zhong, G. Y.; Hou, Y. D.; Liu, J. L.; Shen, B. X. A minireview of viscosity-sensitive fluorescent probes: design and biological applications. *J. Mater. Chem. B* **2020**, *8*, 9642–9651.
[30] Kolanowski, J. L.; Liu, F.; New, E. J. Fluorescent probes for the simultaneous detection of multiple analytes in biology. *Chem. Soc. Rev*. **2018**, *47*, 195–208.
[31] Li, H.; Xin, C. Q.; Zhang, G. B.; Han, X. S.; Qin, W. J.; Zhang, C. W.; Yu, C. M.; Jing, S.; Li, L.; Huang, W. A mitochondria-targeted two-photon fluorogenic probe for the dual-imaging of viscosity and H_2O_2 levels in Parkinson's disease models. *J. Mater. Chem. B* **2019**, *7,* 4243–4251.
[32] Dröge, W. Free radicals in the physiological control of cell function. *Physiol. Rev*. **2002**, *82*, 47–95.
[33] Fan, L.; Wang, X. D.; Ge, J. Y.; Li, F.; Zhang, C. H.; Lin, B.; Shuang, S. M.; Dong, C. A Golgi-targeted off–on fluorescent probe for real-time monitoring of pH changes in vivo. *Chem. Commun*. **2019**, *55*, 6685–6688.
[34] Yin, J. L.; Peng, M.; Lin, W. Y. Visualization of mitochondrial viscosity in inflammation, fatty liver, and cancer living mice by a robust fluorescent probe. *Anal. Chem*. **2019**, *91*, 8415–8421.

Manuscript received: December 29, 2020
Manuscript revised: February 9, 2021
Manuscript accepted: March 4, 2021

 © 2021 SIOC, CAS, Shanghai, & WILEY-VCH GmbH